NASA
Technical
Paper
2480

September 1985

Joint Design for Improved Fatigue Life of Diffusion-Bonded Box-Stiffened Panels

Randall C. Davis,
Paul L. Moses, and
Russell S. Kanenko

NASA

NASA Technical Paper 2480

1985

Joint Design for Improved Fatigue Life of Diffusion-Bonded Box-Stiffened Panels

Randall C. Davis
Langley Research Center
Hampton, Virginia

Paul L. Moses
PRC Kentron, Inc.
Hampton, Virginia

Russell S. Kanenko
Lockheed California Company
Burbank, California

National Aeronautics and Space Administration

Scientific and Technical Information Branch

Summary

Simple photoelastic models were used to identify a cross-section geometry that would eliminate the severe stress concentrations at the bond line between box stiffeners diffusion bonded to a panel skin. Experimental fatigue-test data from titanium test specimens quantified the allowable stress in terms of cycle life for various joint geometries. Results of this research show that the effect of stress concentration was reduced and an acceptable fatigue life was achieved.

Introduction

Feasibility studies for space transportation systems and high-speed aircraft (refs. 1 and 2) have identified structural efficiency as one of the critical technology needs for timely development of these vehicles. Before they can be implemented, efficient structures for such vehicles not only must be identified by analysis but also must be verified by test. For some of these vehicles, the fuselage structure operates at high temperatures and is required to contain an internal pressure as well as carrying the fuselage compressive loads. Optimization techniques (ref. 3) can be used to find efficient, stiffened structures to carry the compressive loads, but the internal pressure induces cyclic tensile loading, transverse to the stiffeners, that will determine the structural fatigue life. Therefore, in addition to carrying the compressive loads without buckling, the efficient stiffened fuselage wall must also demonstrate an adequate cycle life. Mass-strength analyses and system requirements for the present study identified a wall construction with titanium box-stiffened skin (figs. 1 and 2) as a possible candidate for the mass-efficient fuselage of a pressurized vehicle operating in the temperature range of 800°F to 900°F.

To build a prototype of the box-stiffened fuselage wall, recent advances in superplastic forming/diffusion bonding (SPF/DB) fabrication techniques (ref. 4) were used to fabricate a panel as depicted in figure 2. Early test results for the present study from diffusion-bonded prototype panel specimens identified a severe stress-concentration problem at the junction of the box stiffeners and the panel skin due to the lack of filleting in the diffusion-bonded joints. As a result of this stress concentration, the tensile test results indicated the number of cycles to failure for the diffusion-bonded box-stiffened fuselage would be below the desired service life of 10^6 cycles at 50 psi.

Photoelastic models of the stiffener-skin joint were used to quickly identify modifications to the joint that would lower the severity of the stress concentration. Comparison of results from various photoelastic models led to a novel diffusion-bonded joint with a reduced stress concentration. To verify this design, titanium test specimens of this joint were made and tested. Results from fatigue tests of these titanium specimens indicated that the desired cycle life could be achieved at the desired stress level with the box-stiffened skin panel.

The purpose of this report is to describe the results of the photoelastic analysis that led to the modified diffusion-bonded joint design with lower stress concentration. Also presented are the results of the fatigue tests for several titanium stiffener-skin joint configurations.

Test Specimens

The overall geometry for a box-stiffened fuselage panel is shown in figure 1. The components of the box stiffener were preassembled and then the stiffener lower flange with upturned edges was diffusion bonded to the fuselage skin in a separate operation, as depicted in figure 2.

Under the biaxial loading depicted in figure 1, the path of the transverse tensile load encounters a discontinuity as it crosses the stiffener-skin joint. The stress discontinuities thus created are further compounded by the lack of filleting in diffusion-bonded joints. For example, when a simple, flat strip of sheet material is diffusion bonded to a skin, a step discontinuity that has a notch with an essentially zero radius of curvature is produced at the edge of the strip.

Photoelastic Models

Photoelastic models which were 20 times actual size (fig. 3) were cut from a 0.250-in-thick polyurethane sheet. Cuts were made with a high-speed jigsaw, and no further edge finishing was performed. Model A in figure 4, which represented a simple, flat strip bonded to the skin panel, closely duplicated the zero-radius notch at the edge of a strip diffusion bonded to a skin. Model B in figure 4 represented the lower flange of the stiffener bonded to the skin. This model was made to determine the effect of the upturned lower-flange edges on the stress concentration near the sharp notch at the bond junction. Next, it was determined that a chemically milled transition in the skin to form a land area for diffusion bonding the stiffener lower flange would produce a discontinuity with a larger radius. Model C of this chem-milled transition and model D of the chem-milled transition with a bonded lower flange forming an improved doubler were made to assess

this concept. (See fig. 4.) Concerns over the resulting discontinous load path and associated induced bending stresses led to two additional photoelastic models (fig. 5) for assessing the effect of neutral-axis discontinuity on stresses. Model E in figure 5 represented a stiffener-skin joint in which the central part of the land thickness between the upturned edges of the lower flange was reduced to the same thickness as the skin. The sysmmetric photoelastic model F was made to remove the effect of bending stress caused by the discontinous load path. A comparison of results from model E and model F would indicate how severely the bending stresses from an offset neutral axis affect the magnitude of the stress concentrations in the joint.

Titanium Specimens

Sheets of annealed Ti-6Al-4V were superplastically formed to make the individual lower flanges. A single lower flange was then diffusion bonded to an 11-in-wide sheet of annealed Ti-6Al-4V. The sheet and bonded stiffener combination was then cut into several strips transverse to the bond on the stiffener, and the strips were used to make standardized dog-bone fatigue specimens. The various dog-bone fatigue specimens tested are shown in figure 6. Photoelastic models A to D were duplicated in the titanium stiffener-skin specimens illustrated by configurations I to IV in figure 6. Additional specimens, illustrated by configurations V to VII in figure 6, were made to assess the effect of flange overhang and of land height on the cycle life. Configuration VIII was a symmetric version of configuration VII (a set of two configuration VII specimens bonded back-to-back with an aluminum braze alloy) and had no induced bending stresses. The configuration VIII specimen results were used to assess the effect of the induced bending stresses on the configuration VII cycle life.

Test Procedures

Photoelastic Tests

The photoelastic models were mounted in a mechanical loading frame and positioned in a polariscope. Deadweight loading was adjusted so that each specimen carried the same reference stress level of 18 psi in the skin portion of the model. The models were viewed and photographed under collimated, monochromatic light from a mercury-vapor light source. Both the cross-polarizer mode and the parallel-polarizer mode were used in order to identify whole and half fringe locations. Maximum fringe order was determined visually and was used to rank the different specimen geometries relative to each other on the basis of severity of stress concentration.

Titanium Fatigue Tests

The fatigue specimens were positioned in the friction grips of a hydraulic fatigue-test machine. Tensile load cycles were applied at the rate of 30 Hz. The load was alternated between maximum load and 0.1 times maximum load. All testing used to determine the cycles to failure for the various types of joints was done at room temperature (72°F).

Results and Discussion

Photoelastic Tests

Photoelastic model A of the standard doubler under a tensile load showed a severe stress concentration at the bottom of the notch (fig. 4). Model B of the flanged doubler, also shown in figure 4, showed a stress concentration that was also unacceptable. Photoelastic model C, a chem-milled transition with a generous radius, showed a stress concentration that was greatly reduced by the large-radius transition. Photoelastic model C illustrated an area of nearly zero stress at the raised corner of the land (fig. 4). Model D duplicated a proposed joint that would diffusion bond the stiffener lower flange to the chem-milled transition such that the bond line ended at the corner of the land, where the stresses were at their lowest. Results from model D, the improved doubler joint, showed that this location for the sharp notch of the lower-flange–skin joint was out of the area of stress concentration that affected the cycle life.

Results from photoelastic model D of the improved doubler joint also illustrated that the tensile load path across the stiffener was not straight and that a bending moment was induced in the skin and stiffener combination. This bending moment was a result of the offset between the neutral axis of the thicker land material and the neutral axis of the skin. This bending moment produced bending stresses that could have had an adverse effect on the cycle life. Reducing the land thickness of the chem-milled transition between the stiffener lower-flange edges, leaving a small land width only at each edge of the stiffener as in model E of figure 5, helped reduce the load path mismatch and the severity of the bending stresses. However, to assess the effects of the bending stresses on the stress concentration, photoelastic results from model E were compared with results from a symmetric version of this specimen (model F of fig. 5). The symmetric model F had a continuous straight neutral axis and, hence, no

induced bending stresses. Comparing results from models D, E, and F showed that reducing the land thickness reduced stress concentrations to near the order of the symmetric specimen. Although the bending was significantly reduced, a new but lower level of stress concentration was introduced inside the reduced land portion of the joint. The effect of this stress concentration on cycle life was studied with the titanium specimens.

Titanium Fatigue Tests

The cyclic fatigue-test results from the titanium specimens matching the photoelastic models are shown in figure 7. Figure 7 is a standard stress-level and cycle-life plot. Testing was stopped between 10^6 and 10^7 cycles for specimens that did not fail. Results for configuration I specimens of a simple strip diffusion bonded to a sheet, which identified the stress concentration problem, are indicated by the diamond-shaped symbols in figure 7. Results for configuration II specimens of a lower flange with upturned edges bonded to a sheet are indicated by the square-shaped symbols in figure 7. The configuration II specimens had a cycle life of less than 10^6 cycles at 50 ksi. Results from the configuration III specimens of a chem-milled transition are indicated by the circular symbols in figure 7 and indicate a cycle life of 10^6 cycles at a stress level of 66 ksi. Configuration IV specimens combined a chem-milled transition under a bonded lower flange to form an improved doubler joint. The configuration IV results are indicated by the triangular symbols and show a cycle life of 10^6 cycles at slightly less than 50 ksi. This was a considerable improvement over configurations I and II but was still slightly short of an acceptable level. To complete the design study, refinements were investigated to try to achieve the desired cycle life of 10^6 cycles at 50 ksi.

Refinements of the improved doubler joint design in specimen IV consisted of introducing various land thicknesses and lower-flange overhangs in configurations V, VI, and VII as shown in figure 6. The fatigue-test results for these specimens are shown in figure 8. The chem-milling process produced a step radius that was approximately twice the step height from the skin thickness to the land thickness. By comparing the results in figure 8, it is noted that a thinner land thickness and an overhang of the lower flange produced the best results. The lack of a lower-flange overhang, as used in configuration V, resulted in a lower working stress level than was achieved with an overhang. In configuration VI, the size of the step and the radii were doubled over that of the configuration IV but resulted in a lower working stress level than either configuration IV or V. This implies that a more severe stress concentration existed in configuration VI than in configuration IV because of higher induced bending stresses in the joint as a result of the greater mismatch between the neutral axes of the skin and the skin—lower-flange joint section. The combined refinements of a 0.015-in-land thickness and an overhanging lower flange in configuration VII produced the desired cycle life of 10^6 cycles at the 50 ksi stress level. (See fig. 9.)

Fatigue results from configuration VII specimens and its symmetric counterpart, configuration VIII, are shown in figure 9. Configuration VI results from figure 8 are repeated in figure 9 for comparison. The symmetric configuration VIII results show that the absence of bending stresses improved the cycle life at the higher stress levels. However, for the longer cycle-life values, the symmetric configuration VIII did not perform as well as the single-sided configuration VII. The slightly lower endurance strength in the configuration VIII specimens was due to a shift in the failure mode to outside of the test area, as can be seen in figures 10 and 11. Since the configuration VIII specimen was made by diffusion bonding two configuration VII specimens, the sheet portion of the configuration VIII specimen consisted of a layer of titanium bonded with aluminum braze alloy to another layer of titanium rather than a single sheet of titanium. Microstructural analysis of this bond line in these failure zones revealed the formation of brittle intermetallic titanium-aluminum compounds and voids at the interface of the titanium and the aluminum braze in the bond line. Such failure mechanisms are incidental to the objective in these tests. It is believed that higher endurance strengths would have been achieved at the higher cycle-life values if the voids and aluminum in the bond line was not present. Based on the higher stress level results from the symmetric configuration VIII specimens at the lower cycle-life values, a reduction in bending stresses across the joint has been shown to improve the working stress level by about 10 percent over that demonstrated by the single-sided configuration VII specimens.

Conclusions

Simple photoelastic models were used to identify a cross-section geometry that would eliminate the severe stress concentrations at the bond line between box stiffeners diffusion bonded to a panel skin. The photoelastic model of a chem-milled land revealed a region of low stress at the corner of the land, which provided an excellent location for the bond line of the stiffener-skin joint. The photoelastic-model results verified a reduced stress concentration in a combined chem-milled-step and diffusion-bonded-stiffener joint. Additionally, the photoelastic-model

results showed that reducing the thickness of the land under the stiffener reduced the induced bending stresses caused by a discontinuous load path and reduced the stress concentration for this improved doubler joint design.

Titanium fatigue specimen results demonstrated a potentially significant loss in fatigue life associated with the stress concentrations found with the photoelastic models. Titanium fatigue specimens with varying geometric details for the improved doubler joint design showed that increased land depth and no flange overhang increased bending stresses in the joint, adversely affecting cycle life. A refined joint with a flange overhang and a thin land thickness gave a joint that provided the desired cycle life of 10^6 cycles at 50 ksi. Results from symmetric specimens showed that further reductions in load path discontinuity could improve the cycle life to 10^6 cycles at stresses greater than 50 ksi.

NASA Langley Research Center
Hampton, VA 23665-5225
June 5, 1985

References

1. Taylor, Allan H.; Jackson, L. Robert; Davis, Randall C.; Cerro, Jeffrey A.; and Scotti, Stephen J.: Structural Concepts for Future Space Transportation Orbiters. AIAA-83-0210, Jan. 1983.
2. Kelly, H. Neale; and Gardner, James E., compilers: *Advances in TPS and Structures for Space Transportation Systems.* NASA CP-2315, 1984.
3. Anderson, Melvin S.; and Stroud, W. Jefferson: A General Panel Sizing Computer Code and Its Application to Composite Structural Panels. *AIAA J.*, vol. 17, no. 8, Aug. 1979, pp. 892–897.
4. Bales, Thomas T., ed.: *SPF/DB Titanium Technology.* NASA CP-2160, 1980.

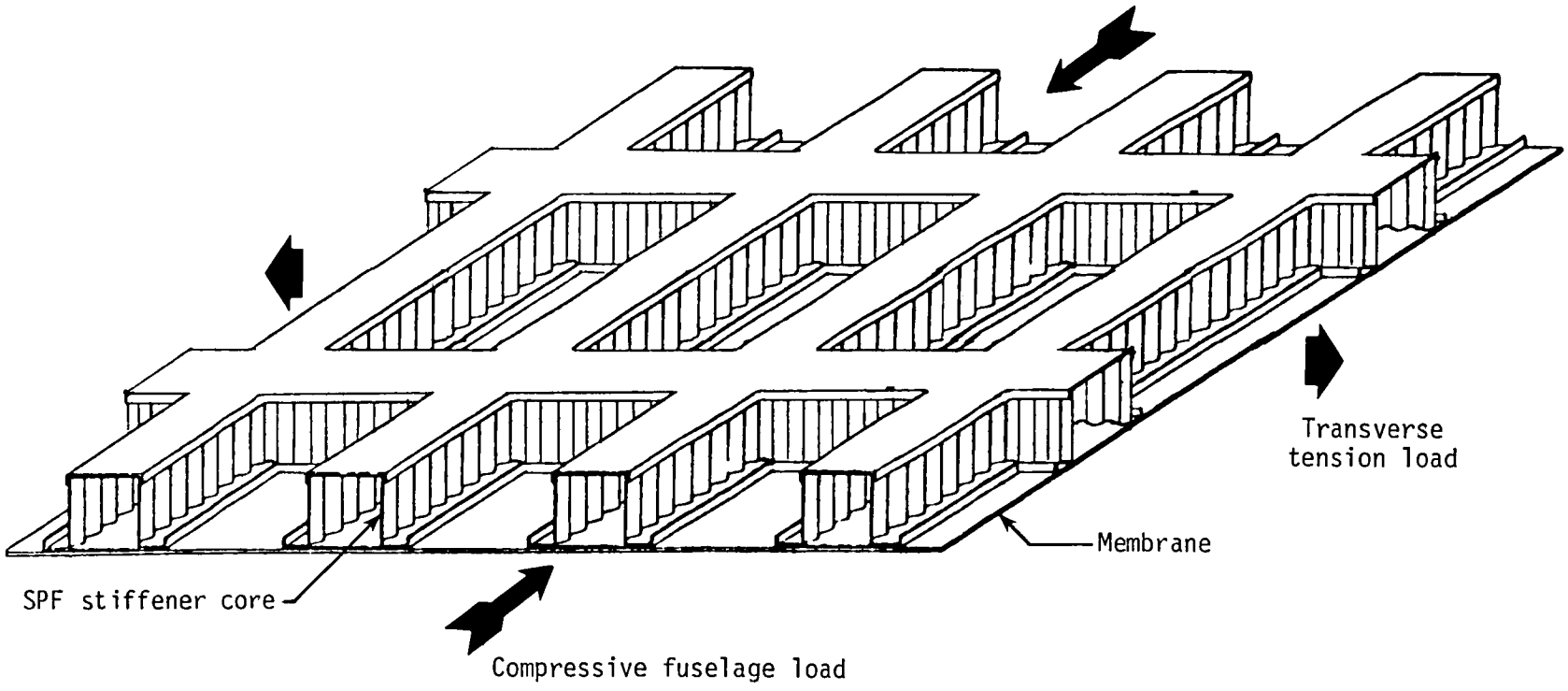

Figure 1. General construction of box-stiffened fuselage wall and its loads.

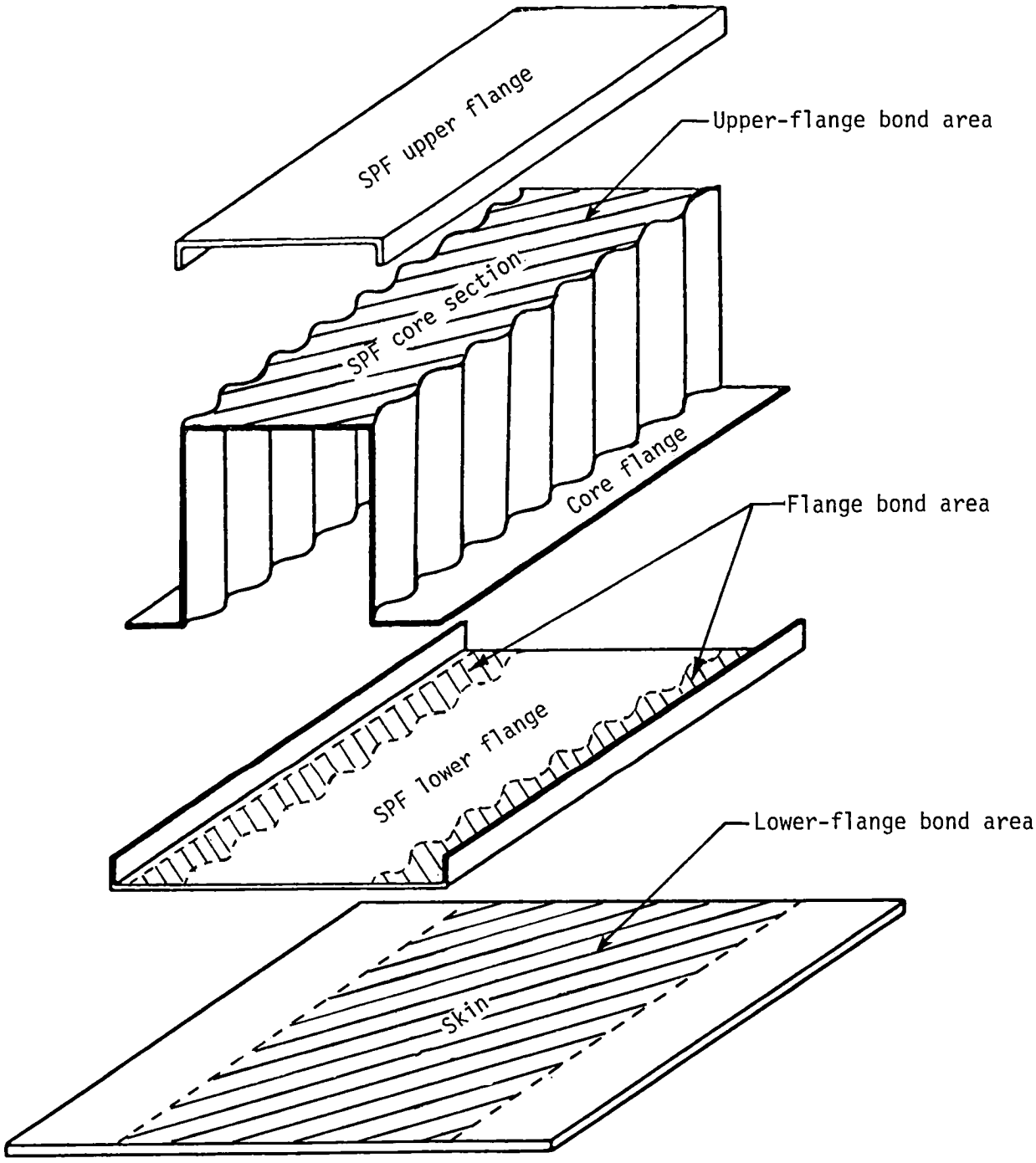

Figure 2. Exploded view of component parts of box-stiffened panel.

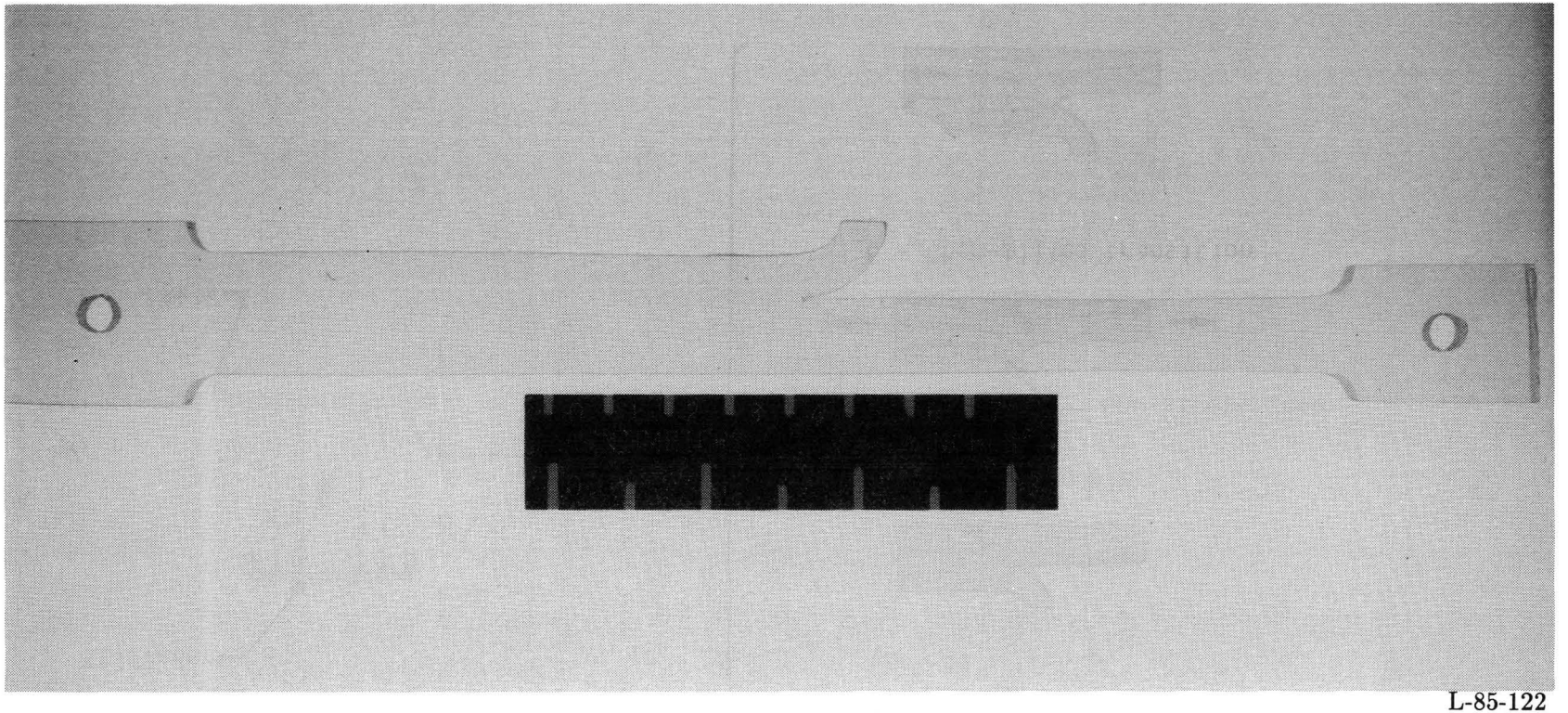

L-85-122

Figure 3. Sample of photoelastic specimen 20 times actual size.

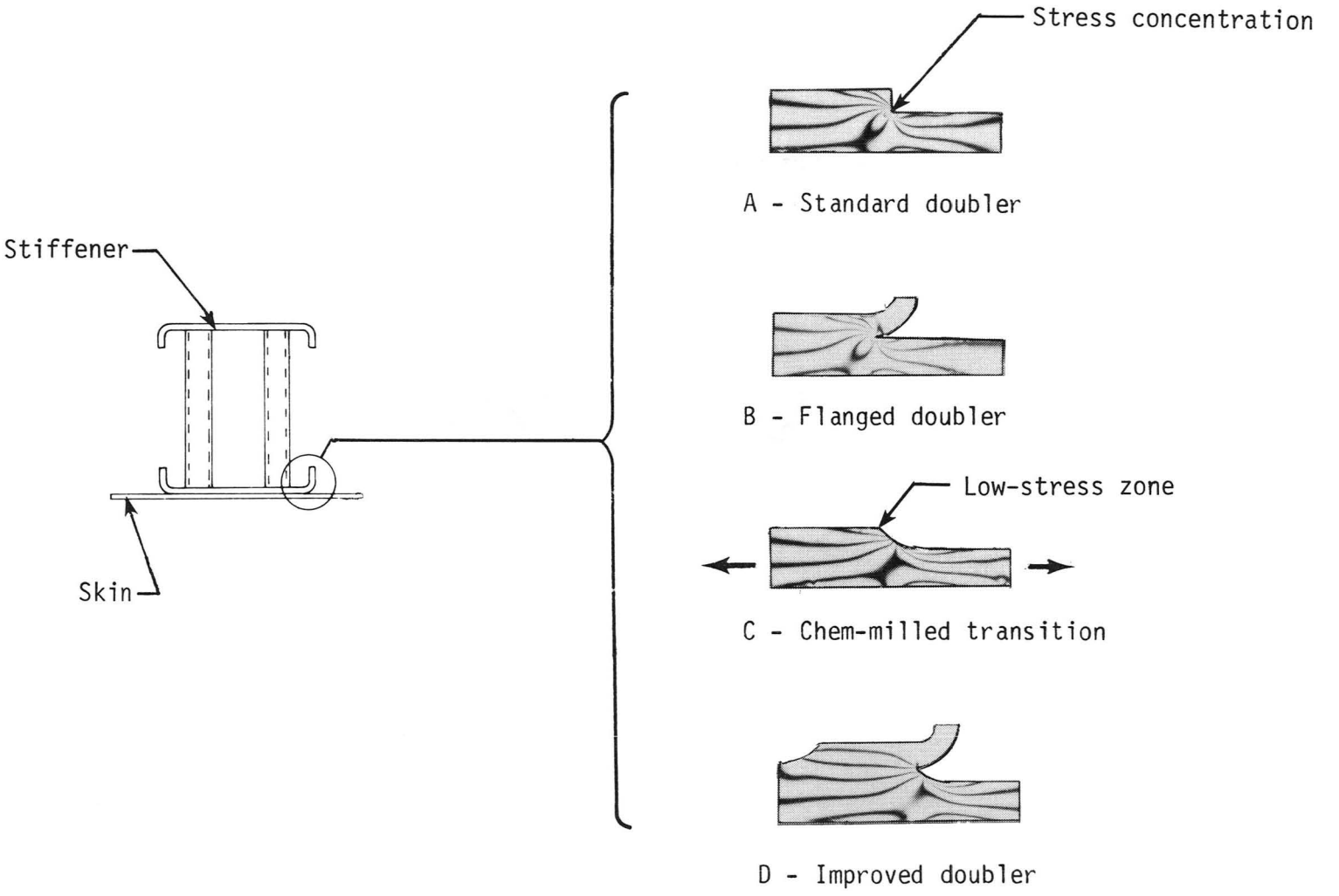

Figure 4. Various photoelastic models of stiffener-skin joints.

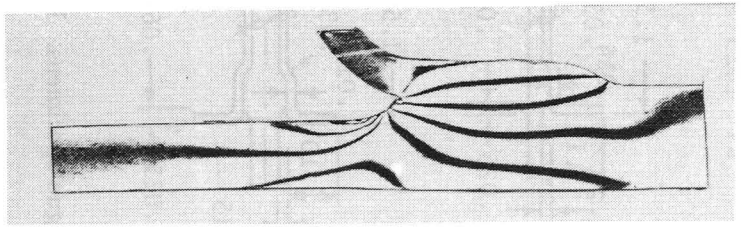

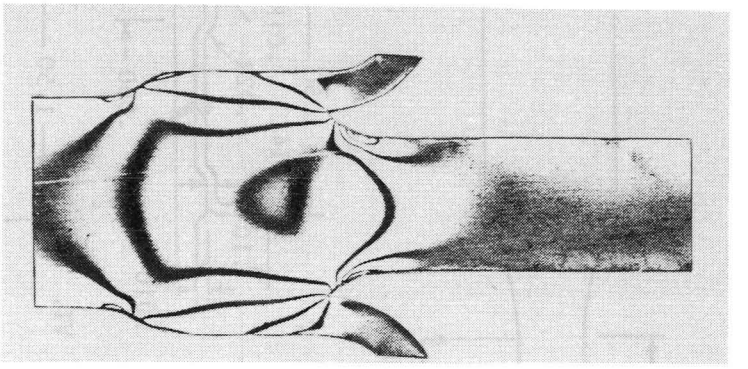

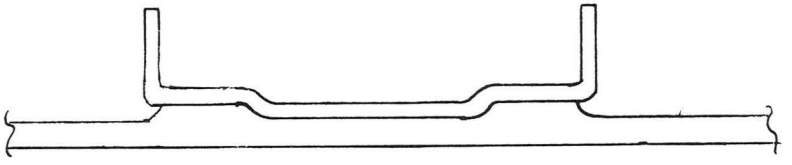

E - Improved doubler with reduced land

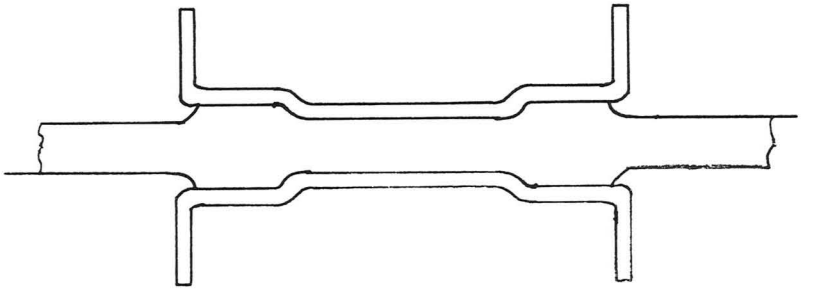

F - Symmetric improved doubler

Figure 5. Stiffener-skin joint configurations for comparing reduced bending stresses in joint.

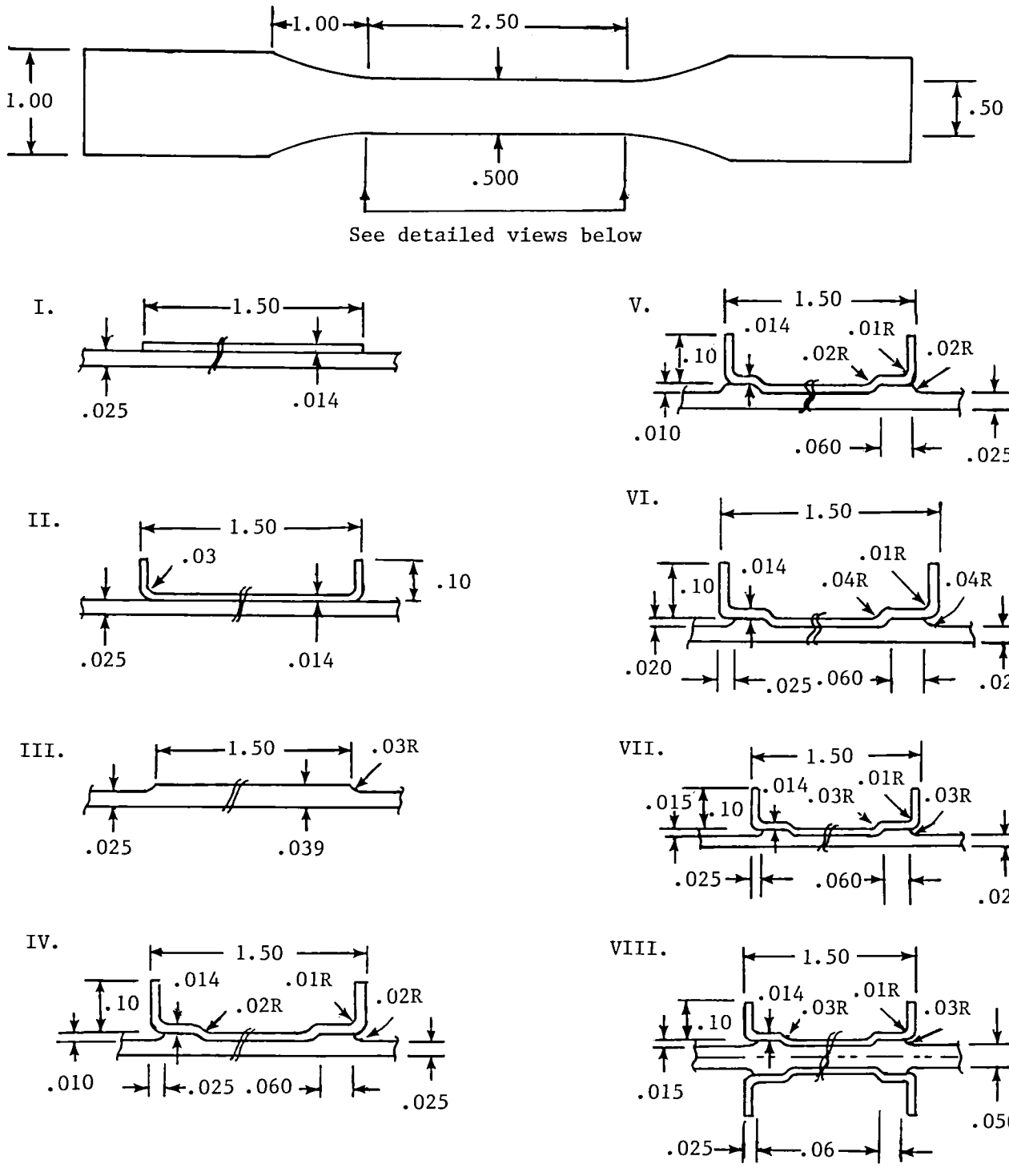

Figure 6. Geometric details of the annealed Ti-6Al-4V dog-bone fatigue specimens. Radii of curvature are indicated by R. All dimensions are in inches.

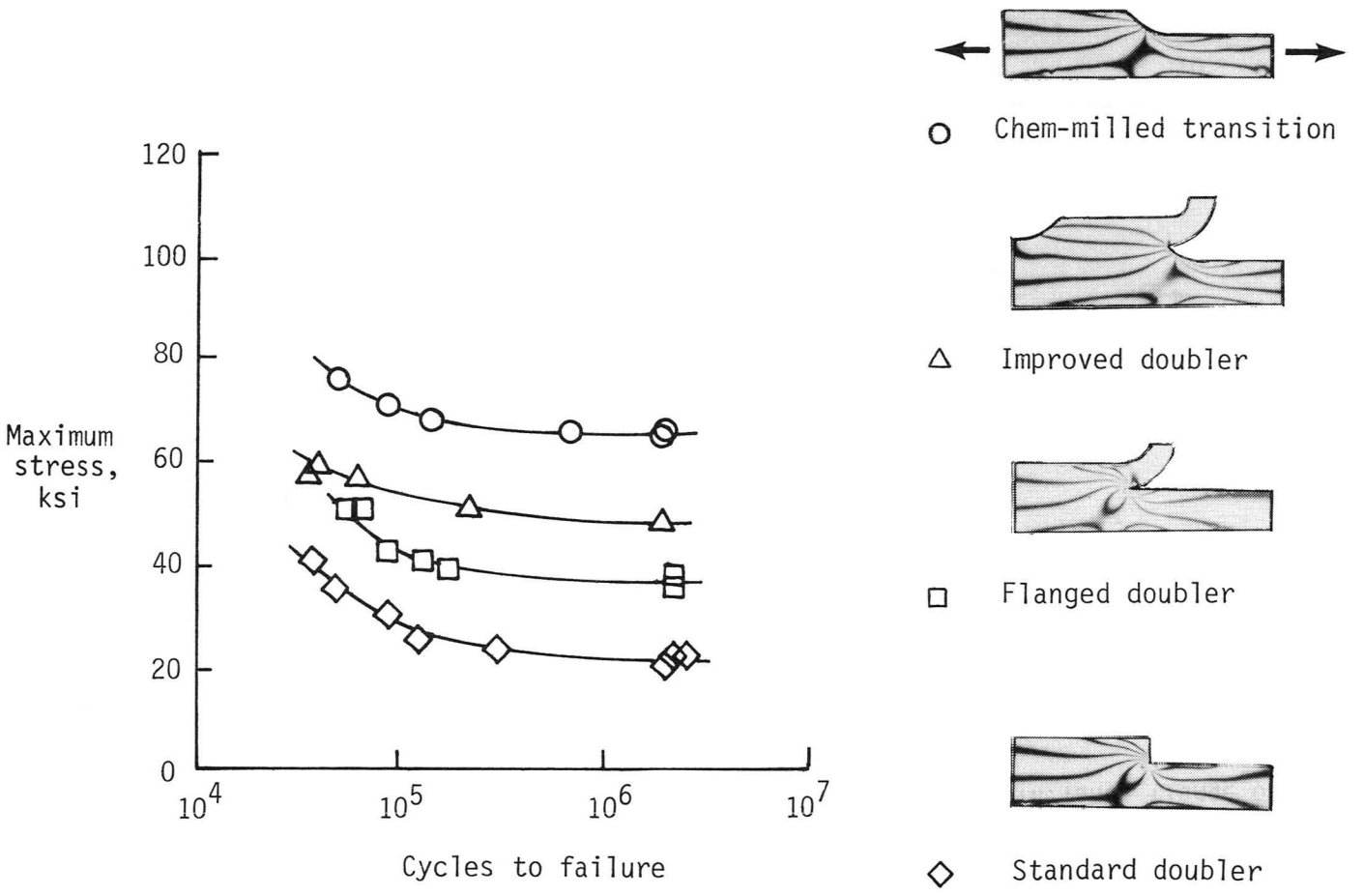

Figure 7. Fatigue-test results for specimens of configurations I to IV.

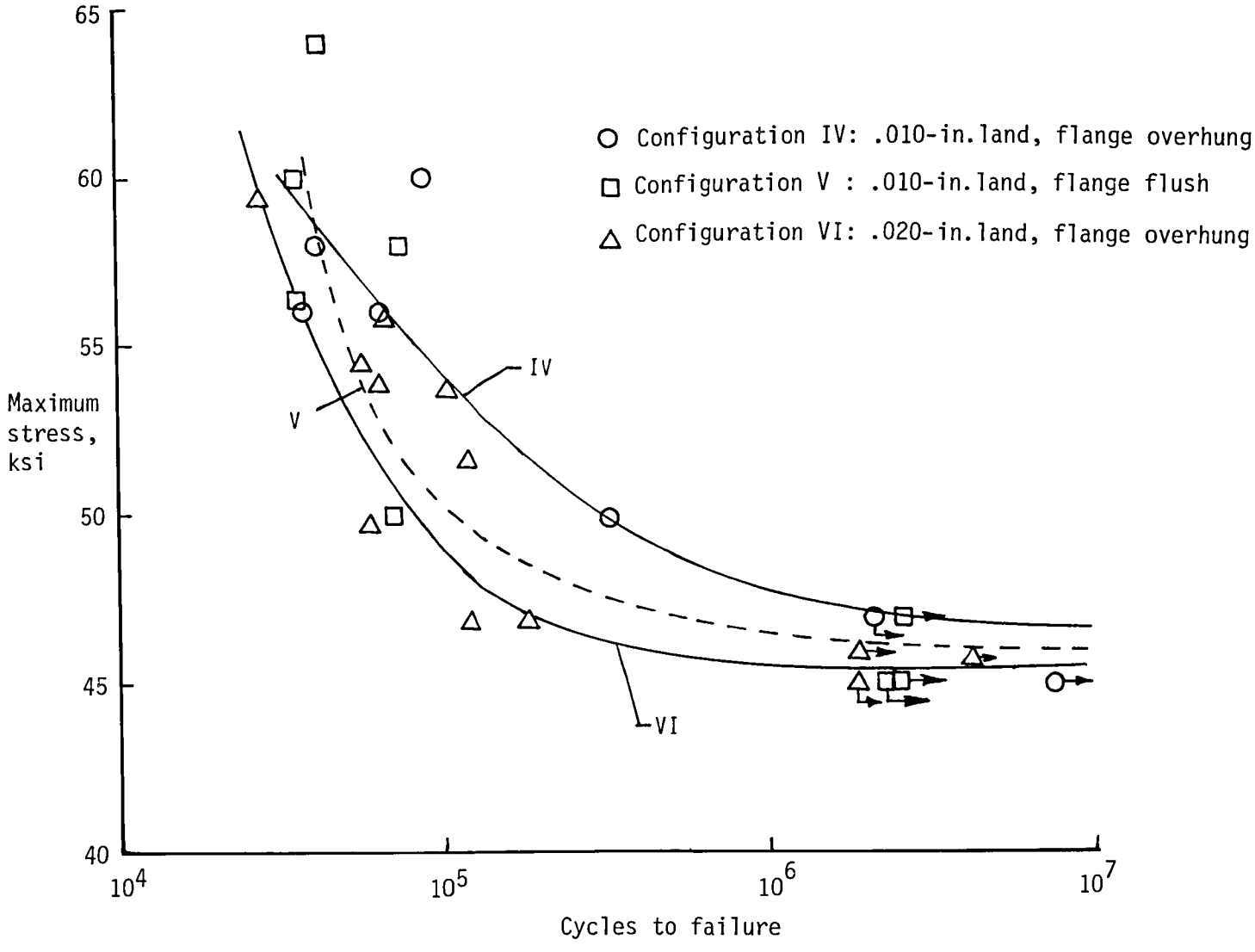

Figure 8. Fatigue-test results for specimens of configurations IV to VI. (Arrows on the symbols indicate runout.)

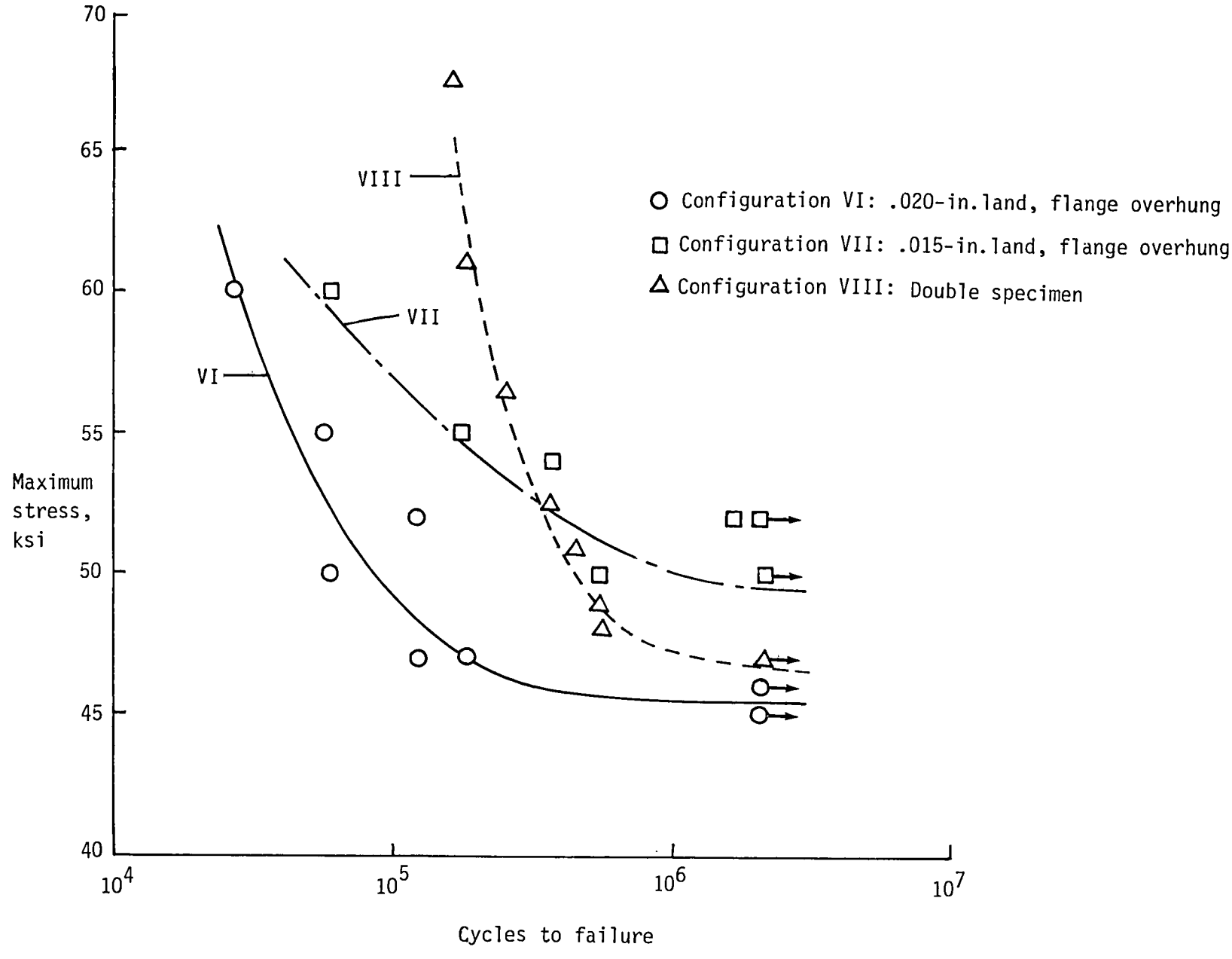

Figure 9. Fatigue-test results for specimens of configurations VII to VIII. (Arrows on symbols indicate runout.)

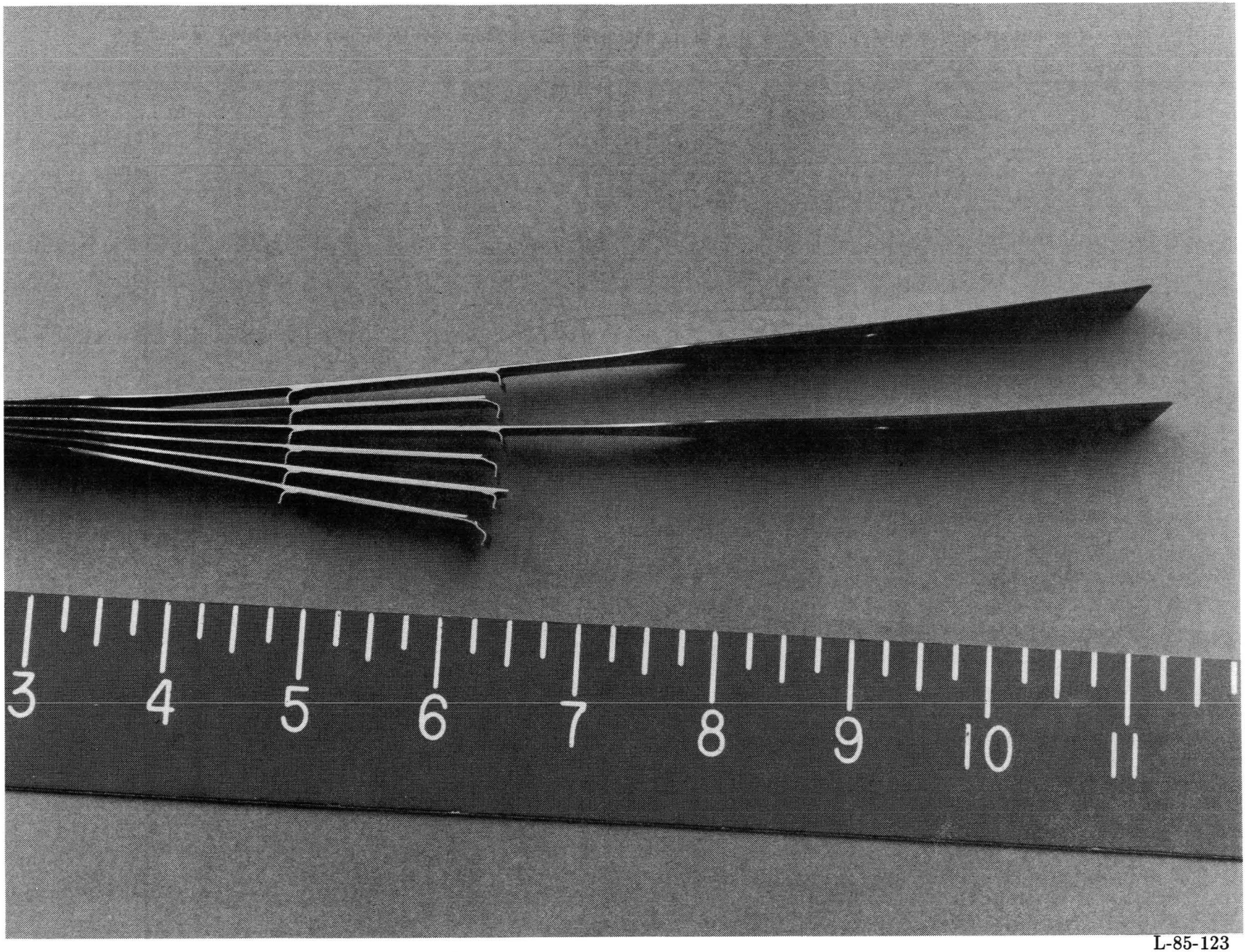

L-85-123

Figure 10. Typical failed configuration VII fatigue specimen.

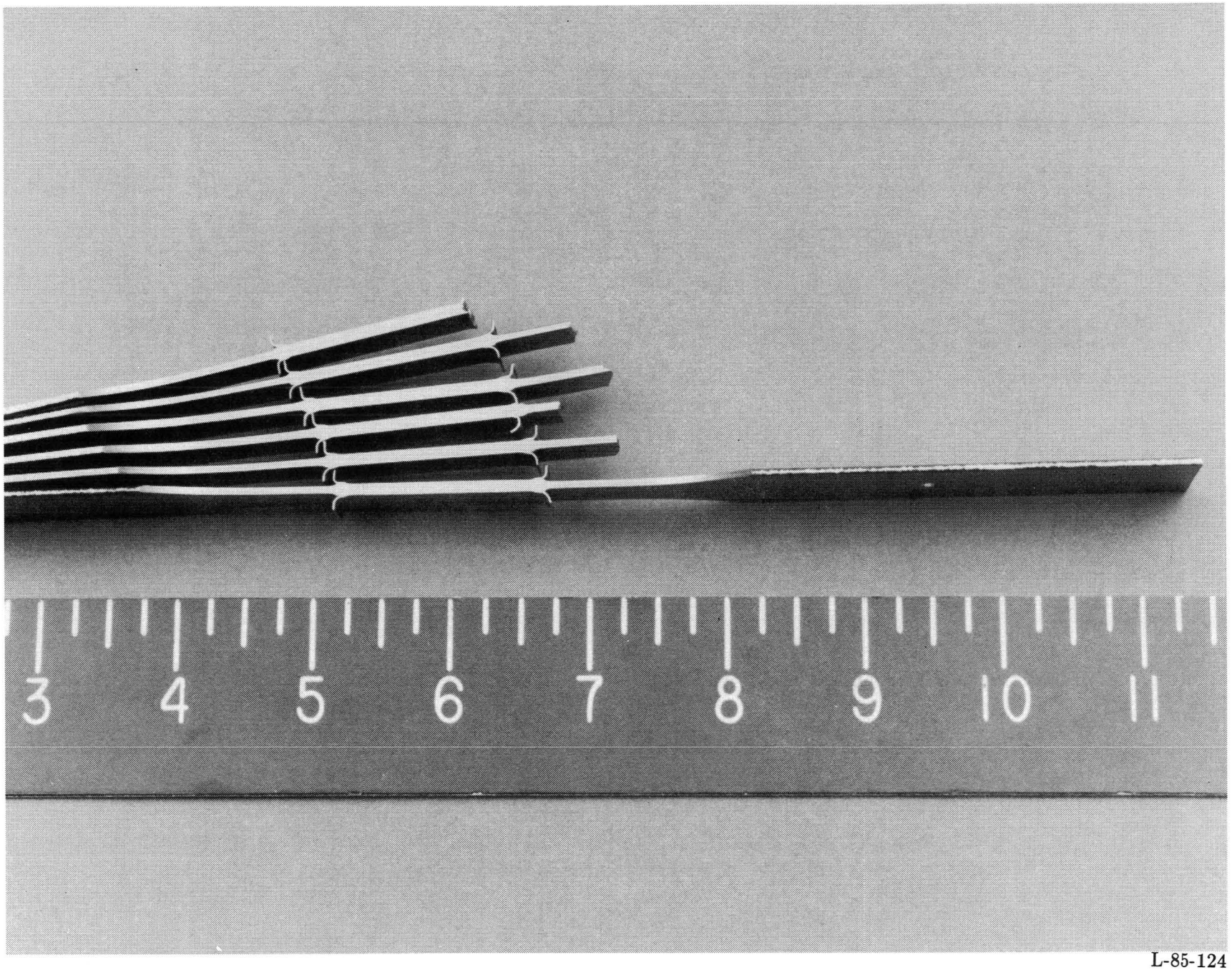

L-85-124

Figure 11. Typical failed configuration VIII fatigue specimen.

Standard Bibliographic Page

1. Report No.	2. Government Accession No.	3. Recipient's Catalog No.
NASA TP-2480		

4. Title and Subtitle	5. Report Date
Joint Design for Improved Fatigue Life of Diffusion-Bonded Box-Stiffened Panels	September 1985
	6. Performing Organization Code: 506-53-33-11
7. Author(s): Randall C. Davis, Paul L. Moses, and Russell S. Kanenko	8. Performing Organization Report No.: L-15967
9. Performing Organization Name and Address: NASA Langley Research Center, Hampton, VA 23665-5225	10. Work Unit No.
	11. Contract or Grant No.
12. Sponsoring Agency Name and Address: National Aeronautics and Space Administration, Washington, DC 20546-0001	13. Type of Report and Period Covered: Technical Paper
	14. Sponsoring Agency Code

15. Supplementary Notes

Randall C. Davis: Langley Research Center, Hampton, Virginia.
Paul L. Moses: PRC Kentron, Inc., Hampton, Virginia.
Russell S. Kanenko: Lockheed California Co., Burbank, California.

16. Abstract

Simple photoelastic models were used to identify a cross-section geometry that would eliminate the severe stress concentrations at the bond line between box stiffeners diffusion bonded to a panel skin. Experimental fatigue-test data from titanium test specimens quantified the allowable stress in terms of cycle life for various joint geometries. Results of this research show that the effect of stress concentration was reduced and an acceptable fatigue life was achieved.

17. Key Words (Suggested by Authors(s))	18. Distribution Statement
Stiffened panel Diffusion bond Fatigue life Test Photoelasticity Titanium Optimization Compression Buckling	Unclassified—Unlimited Subject Category 39

19. Security Classif.(of this report)	20. Security Classif.(of this page)	21. No. of Pages	22. Price
Unclassified	Unclassified	16	A02

For sale by the National Technical Information Service, Springfield, Virginia 22161

NASA-Langley, 1985

National Aeronautics and
Space Administration

Washington, D.C.
20546

Official Business
Penalty for Private Use, $300

BULK RATE
POSTAGE & FEES PAID
NASA Washington, DC
Permit No. G-27

NASA

POSTMASTER: **If Undeliverable (Section 158 Postal Manual) Do Not Return**